Available on CMS information server

CMS CR -2010/011

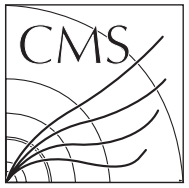

The Compact Muon Solenoid Experiment

Conference Report

Mailing address: CMS CERN, CH-1211 GENEVA 23, Switzerland

14 January 2010 (v2, 26 January 2010)

Measurement of The Muon Stopping Power in Lead Tungstate

Andrea Davide Benaglia for the CMS Collaboration

Abstract

During October-November 2008 the CMS Collaboration conducted a data-taking exercise in order to complete the commissioning of the experiment for extended operation. A large sample of cosmic ray triggered events has been recorded with the solenoid at its nominal axial field strength of 3.8 T. The events collected have been exploited to perform a measurement of specific energy loss of muons in lead tungstate - the electromagnetic calorimeter material - over a wide momentum range (from 5 GeV/c to 1 TeV/c). The results are consistent with the expectations over the entire range. A comparison of collision losses with radiative losses allowed for a first experimental determination of muon critical energy in lead tungstate, measured to be $160^{+5}_{-6} \pm 8$ GeV, in agreement with expectations.

Presented at *SIF 2009: XCV congresso nazionale dell Società Italiana di Fisica*

Measurement of The Muon Stopping Power in Lead Tungstate

A. Benaglia([1])([*]) for the CMS Collaboration

([1]) *Università degli Studi di Milano - Bicocca and INFN - Piazza della Scienza 3, Milano, Italy*

(ricevuto ?)

Summary. — During October-November 2008 the CMS Collaboration conducted a data-taking exercise in order to complete the commissioning of the experiment for extended operation. A large sample of cosmic ray triggered events has been recorded with the solenoid at its nominal axial field strength of 3.8 T. The events collected have been exploited to perform a measurement of specific energy loss of muons in lead tungstate - the electromagnetic calorimeter material - over a wide momentum range (from 5 GeV/c to 1 TeV/c). The results are consistent with the expectations over the entire range. A comparison of collision losses with radiative losses allowed for a first experimental determination of muon critical energy in lead tungstate, measured to be $160^{+5}_{-6} \pm 8$ GeV, in agreement with expectations.

1. – Introduction

While waiting to record events from beam collisions at the LHC, the electromagnetic calorimeter (ECAL) of the Compact Muon Solenoid (CMS) experiment has been exploited to measure the muon stopping power in the lead tungstate of its crystals for cosmic ray muon momenta between 5 and 1000 GeV/c.

The stopping power for muons in the energy range considered can be conveniently written as

$$f(E) = \left\langle -\frac{\mathrm{d}E}{\mathrm{d}x} \right\rangle = a(E) + b(E)E\,,$$

where E is the total muon energy, x is the thickness of the traversed material, commonly measured in mass per unit surface, $a(E)$ is the stopping power due to collisions with atomic electrons, and $b(E)$ is due to radiative processes: bremsstrahlung, direct pair production, and photonuclear interactions; $a(E)$ and $b(E)$ are slowly varying functions of E at energies where radiative contributions are important [11, 9].

([*]) andrea.benaglia@mib.infn.it

Numerical values of stopping power and related quantities quoted throughout this paper are taken from tables in [12]. The tables (see [11]) are obtained from calculations following [9, 10]. The theoretical uncertainties are everywhere smaller than the statistical precision of the results in this analysis.

The definition of critical energy as the energy at which the average rates of energy loss through collision and radiation are equal [11, 9] is adopted in this paper. Analysis of data in the full momentum range permits a comparison of collision losses with radiative losses, thus leading to the first experimental determination of muon critical energy.

The experimental setup and the characteristics of the data sample are described in Section **2**. Measurement of relevant physical quantities and event selection are discussed in Section **3**. Possible limitations in the measurement of the muon stopping power are addressed in Section **4**. In Section **5**, corrections for systematic effects and statistical issues are addressed, and results are reported.

2. – Experimental setup

The central feature of the CMS detector is a superconducting solenoid of 6 m internal diameter, providing a field of 3.8 T. Within the field volume are the silicon pixel and strip tracker, the crystal electromagnetic calorimeter and the brass-scintillator hadron calorimeter (HCAL). Muons are measured in gas-ionization chambers embedded in the steel return yoke. In addition to the barrel and endcap detectors, CMS has an extensive forward calorimetry. For a much more detailed description of CMS, see [1].

The silicon pixel and strip detectors provide excellent momentum reconstruction, with a 10 % resolution for 1 TeV/c muons passing close to the nominal interaction vertex.

The electromagnetic calorimeter is a hermetic homogeneous scintillator detector made of lead tungstate ($PbWO_4$) crystals. Lead tungstate has a high density (8.3 $\mathrm{g\,cm^{-3}}$), a short radiation length, ($X_0 = 0.89$ cm) and a small Molière radius ($R_M = 2.0$ cm). Crystals are organized in a central barrel of 61 200 crystals closed by two end-caps of 7324 crystals each. The light is read out by avalanche photodiodes (APD) in the barrel and by vacuum phototriodes (VPT) in the end-caps. In the barrel, relevant to the analysis here presented, the individual crystals have a truncated-pyramid shape with a mean lateral size in the front section of 2.2 cm and a length of 23 cm, which corresponds to 25.8 radiation lengths. The barrel crystals are organized in a quasi-projective geometry, where their principal axis is tilted by 3° with respect to the nominal interaction vertex, in both the azimuthal and polar angle projections.

In October-November 2008 all installed detector systems participated to a month-long data-taking campaign known as CRAFT([1]), with the goal of commissioning the experiment for extended operation [2]. The 270 million cosmic ray triggers collected consist of muons traversing the CMS detector in its final configuration in the experimental cavern, located 100 m underground.

3. – Measurement of physical variables and event selection

The physical variables to be measured for each muon are the momentum (p), the path length in ECAL (Δx), and the energy lost in ECAL (ΔE).

([1]) Cosmic Run At Four Tesla

The muon momentum is measured from the track fit performed in the inner tracking system [4].

The path length in ECAL is estimated by propagating the measured muon track inside the calorimeter taking into account bending due to the magnetic field and expected energy loss. The average path length in ECAL for the selected muon sample is 22.0 cm, from which it follows that the typical energy loss for a minimum ionizing muon is about 300 MeV.

Because of the angular distribution of the cosmic ray muon flux and the lower sensitivity of the ECAL end-caps to the energy released by mip muons, only the barrel part of ECAL is used in the present analysis. The energy deposited in ECAL barrel by cosmic ray muons is measured by means of a dedicated algorithm, specifically designed to provide good reconstruction down to low energy and for deposits originated from muon tracks non pointing to the nominal interaction vertex. For CRAFT runs of interest in this paper, online data reduction is based on zero suppression (ZS), that is, a readout of channels above a ZS threshold of about 20 MeV, and on a full readout of selected regions (SR) of high interest, with a threshold set to about 170 MeV [8]. When the condition for SR is met, a matrix of 3×3 trigger towers is read out. Each tower is comprised of 5×5 crystals and the matrix is centered around the tower with energy deposit above the SR threshold. The energy reconstruction algorithm identifies clusters starting from a central crystal (seed) with an energy deposit of at least 139.5 MeV (or from the most energetic of a pair of adjacent crystals with at least 46.5 MeV each), and adding all the channels above the clustering threshold (18.5 MeV) belonging to a 5×5 matrix of crystals centered on the seed. Contiguous clusters are eventually merged. The final cluster energy is obtained after application of channel-to-channel relative calibration constants and of an absolute energy scale factor, set with data taken with a 120 GeV/c electron beam [6]. Additional corrections, related to noise induced bias and energy containment effects, are addressed in Section **5**.

Clusters in ECAL are associated with muon tracks according to a geometrical match between the track extrapolated to the calorimeter surface and the centre of gravity of the energy deposit.

The initial sample of CMS triggers useful for this analysis is made of 8.8×10^7 events. This sample is reduced by the combined requirements of a muon at the trigger level [5], of a single muon track reconstructed by the tracker [4], and of an energy deposit associated with the track in both the upper and the lower half of ECAL barrel. Since, for the present analysis, the muon momentum has to be measured upstream of the energy release in the calorimeter, only energy deposits in the bottom half of ECAL are used. The upper part of the ECAL barrel is used to veto events with energy deposits above 500 MeV, as it will be clarified in Section **5**. Moreover, the muon momentum is required to be within the range 5-1000 GeV/c, as imposed by the statistics available. Further selections are eventually applied to the event sample: the uncertainty on muon momentum must be smaller than the bin width; the ratio of the energy deposit in the calorimeter to muon momentum must be less than 1 within the experimental accuracy; the angle between the muon track at the ECAL surface and the corresponding crystal axis must be smaller than 0.5 radians. After all requirements, the final sample consists of 2.5×10^5 muons.

The measured muon spectrum, after the selections, is shown in Fig. 1(a). The spectrum of energy deposited in crystals is shown in Fig. 1(b).

Figure 2 displays the distributions of $\Delta E/\Delta x$, the measured cluster energy divided by the path length in ECAL, for muons with momentum below 10 GeV/c, where collision losses dominate (a), and for muons with momentum above 300 GeV/c, where sizable

radiation losses are expected (b).

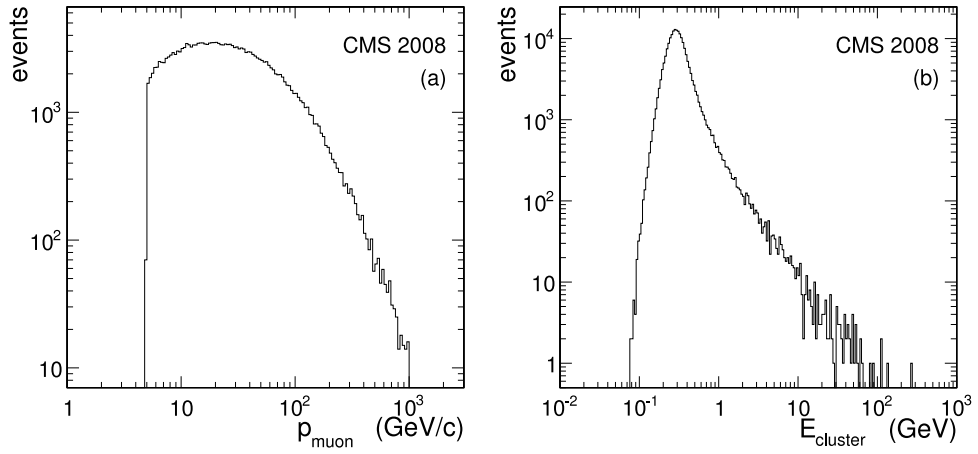

Fig. 1. – (a) Momentum spectrum of the muons passing the selections; (b) spectrum of the reconstructed energy in the lower ECAL hemisphere. A logarithmic binning is used.

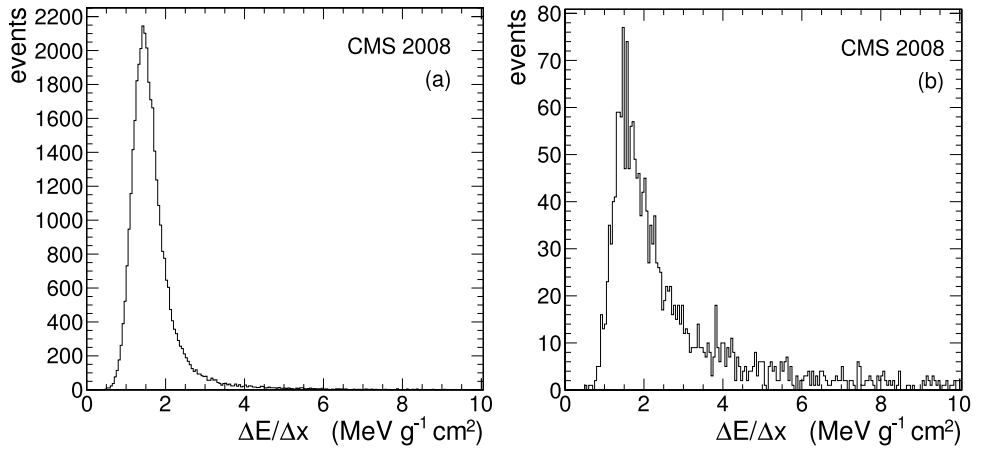

Fig. 2. – Measured distributions of $\Delta E/\Delta x$ in ECAL; (a) for muon momenta below 10 GeV/c; (b) for muon momenta above 300 GeV/c; the fraction of events with $\Delta E/\Delta x > 10$ MeV g^{-1} cm^2 is 1.3×10^{-3} and 8×10^{-2} in (a) and (b) respectively.

4. – Measurement of the stopping power

A calorimetric measurement of the stopping power is determined by the measurement of the energy ΔE lost by a muon when traversing a known thickness Δx. On the one hand, the tickness of material traversed should be large enough to allow a precise measurement of the energy released; on the other, the thickness should be small enough for the variation of the muon energy to be negligible, in order that the approximation $f(E) = -\mathrm{d}E/\mathrm{d}x = \Delta E/\Delta x$ holds. With the present experimental setup, muons cross a thick layer of dense material, Δx being typically 180 g/cm^2 (about 25 X_0 in $PbWO_4$). However it can be shown that $\Delta f/f$, where $\Delta f = f(E) - f(E - \Delta E)$, is everywhere small when compared with other sources of uncertainty.

A second issue to be considered when aiming to measure the muon stopping power is that energy lost by a muon is transferred to energy of secondaries. Since secondaries and their daughters may travel a significant distance, the energy ΔE lost by a muon traversing a given volume is in general different from the energy deposited in that same volume, which is the first output of the measurement procedure. Taking as a reference volume a cylinder with its axis along the muon direction, energy flow across the lateral surface can be made negligible by choosing a sufficiently large radius. On the other hand there is always a non-negligible flow of energy carried by secondaries entering and leaving the two ends of the cylinder, since secondaries are produced along the entire muon path.

In a homogeneous material, an equilibrium between the energy flowing in through the front surface and the energy flowing out of the rear surface is approximately reached when the front surface is preceded by at least an amount of material corresponding to the energy-weighted average range of secondaries. Considering the spectra of secondaries produced by muons, it is found that the equilibrium condition is approached for δ-electrons after the muon has traversed a thickness of about 10 g/cm^2, while for radiated photons about 20 radiation lengths are needed.

In the present case, the experimental setup is well described as a homogeneous region of $PbWO_4$ preceded by order of 10 g/cm^2 of nearby material. Material separated by more than a few tens of centimeters from the crystals is less effective in producing secondaries flowing into the measurement volume because of the presence of a strong magnetic field. Thus the upper half of ECAL barrel has little effect on the energy loss measurement in the lower half of the barrrel. Therefore, net containment corrections are expected to be small or negligible for collision losses, but sizable for radiative losses. A quantitative estimate of these corrections has been obtained by means of a dedicated simulation based on the Geant4 package [7], as detailed in Section **5**.

5. – Data analysis and experimental results

5˙1. *Instrumental effects*. – The relevant instrumental effects are related to the online data reduction and to the energy reconstruction procedure described in Section **3**. The presence of thresholds introduces a bias in energy reconstruction: noise fluctuations above threshold contribute a positive bias, while energy deposits below threshold contribute a negative bias.

When the muon direction is close to the crystal axis (angle beetween muon and crystal axis $\lesssim 0.1$ radians), the condition for SR is met in the majority of cases. The main positive bias then arises from the probability of noise fluctuation above the clustering threshold. A 14.7 MeV bias is estimated by means of a dedicated analysis of the noise spectrum.

At larger muon angles to the crystal axis, the crystal multiplicity in cluster increases

and the average energy deposit per crystal decreases correspondingly. Therefore conditions for ZS read-out occur more frequently, with the higher ZS threshold reducing the noise bias. Moreover, the probability that the energy deposited in a single crystal is below clustering threshold increases, thus contributing a negative bias. Bias is then expected to decrease with increasing angles.

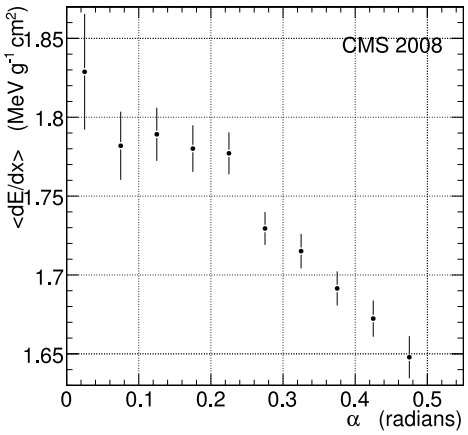

Fig. 3. – Dependence of the raw $\langle \mathrm{d}E/\mathrm{d}x \rangle$ on the angle α between the muon direction and the crystal axis, for muon momentum between 5 and 10 GeV/c. Vertical bars represent statistical errors.

This bias dependence on angle for non-radiating muons is observed in experimental data, as shown in Fig. 3, where the raw measured $\mathrm{d}E/\mathrm{d}x$ is displayed versus angle for muons below 10 GeV/c.

A bias correction is thus applied to the estimated collision component of the stopping power by applying the following procedure. At small angles, a bias of 14.7 MeV is subtracted. At larger angles, the bias to be subtracted is estimated from a fit to the data shown in Fig. 3. The uncertainty in the evaluation of the 14.7 MeV bias and the statistical uncertainty of the fit contribute to the systematic uncertainty of the bias correction, yielding an overall systematic uncertainty of 3.5 MeV, which corresponds to about 1.2 % of the average energy deposited by a low-momentum muon.

The bias is estimated to be negligible for larger energy deposits from radiating muons; it is in any case negligibly small compared to the systematic effects discussed in Section **5**˙2. Therefore, no bias correction is applied to the radiative component of the stopping power over the entire muon momentum spectrum.

5˙2. *Containment corrections.* – To estimate the difference between energy lost and energy deposited in ECAL, a model based on the Geant4 simulation toolkit, with a simplified description of the detector and materials surrounding it, was developed. Since only nearby material is effective in producing secondaries flowing into measurement volume, as explained in Section **4**, the upper half of the ECAL has been ignored in the simulation. The validity of this approximation has been reinforced by selecting, in the analysis, only muons that produce a signal of less than 500 MeV in the upper part of the ECAL, thus removing most of those emitting a hard photon.

Energy leakage and the effects of upstream and downstream materials are quantitatively different for collisions and radiative processes; therefore, the low-momentum and the high-momentum regions have been treated separately.

The low-momentum region is of major interest for the present analysis, since the large sample size and the small energy loss fluctuations allow precise results to be obtained. According to the simulation, the energy carried by secondaries flowing out of the rear detector surface is, on average, 3 % of the energy lost in the crystals for a muon with momentum 15 GeV/c. This represents an upper limit to containment corrections in the low-momentum region, since the rear leakage can be compensated by secondaries produced in upstream material entering the front detector surface (see Section **4**). A comparison of the deposits in the upper and lower hemispheres of the ECAL barrel, for muons with momentum between 5 and 10 GeV/c, shows no difference in $\mathrm{d}E/\mathrm{d}x$, with a sensitivity better than 1 % [3]. Given this result, in spite of the asymmetric distribution of the outer and inner material around ECAL, containment correction has been neglected, and 1 % systematic uncertainty on the null correction has been assumed for collision losses.

Energy containment corrections in the high-momentum region have been derived from dedicated simulations of two extreme cases: with no material in front of ECAL and with the whole material budget of the tracker concentrated just in front of ECAL. The former case represents the upper limit to the containment correction, where only rear losses are considered; the latter case gives a lower limit to the correction, as it maximally overestimates the energy flow through the front face due to upstream material. The mean value and half of the difference between the results of the two simulations are the estimate of the corrections for the energy containment in radiative processes and of the associated systematic error. The correction is maximal at 1 TeV/c and corresponds to (28 ± 5) % of the average energy lost, while at 170 GeV/c it reduces to (14.5 ± 2.5) %. Such an uncertainty is small compared to the statistical uncertainty in the measurement of the stopping power in radiative region. The correction for non-containment of radiated secondaries is applied over the whole momentum spectrum to the expected contribution of radiative processes to stopping power.

5˙3. *Energy scale and critical energy.* – In Fig. 4(a), the specific muon energy loss resulting after corrections is compared to expectations as a function of the muon momentum [12]. Fig. 4(b) shows the ratio of experimental measurements to expected values. Two regions are indicated in Fig. 4: the expected 68 % probability central interval (grey shaded area), and the minimum interval corresponding to 68 % probability (region delimited by continuous curves). The reasons for considering both intervals and the procedure adopted for their estimate are summarized below.

Radiative losses are rare events characterized by large energy releases. As a consequence, the probability density functions (pdf) of energy loss for single events are positively skewed distributions, with long tails at high energy. The skewness of the single event pdf increases with increasing muon momentum, owing to the increasing contribution of radiative processes with momentum. At the same time, the number of events per bin in the selected data sample rapidly decreases with momentum for $p > 50$ GeV/c (Fig. 1(a)). It is thus expected that, due to the combination of these two effects, the pdf of the sample mean of $\mathrm{d}E/\mathrm{d}x$ cannot be approximated by a Gaussian in the higher momentum bins. Moreover, when this condition occurs, sample mean and sample variance are highly correlated. It follows that the widely used "experimental error", namely the sample rms divided by the square root of the sample population, is not a good measure

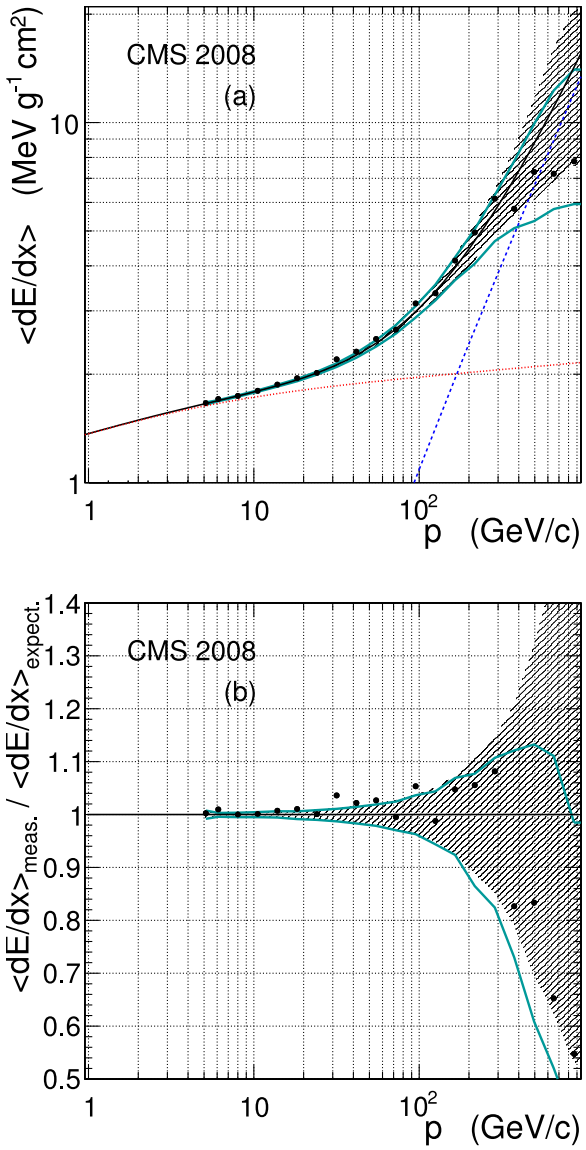

Fig. 4. – (a) Muon stopping power measured in $PbWO_4$ (dots) as a function of muon momentum compared to expectations [12] (continuous line). The expected contributions from collision and radiative processes are plotted as well (dotted line and dashed line respectively). (b) Ratio of the measured and the expected values of the muon stopping power, as a function of muon momentum. As discussed in the text, in both figures, the shaded grey area indicates the expected 68 % probability central interval, while the continuous curves delimit the minimum interval containing 68 % of the expected results. "Experimental errors" are not shown for reasons discussed in the text.

for the consistency of the sample mean with the expected value.

Therefore the uncertainty of the result has been estimated by means of a numerical technique based on the simulation of the expected results with Geant4. Ten thousand pseudo-experiments per momentum bin, each with the same statistics as the actual bin population, were simulated. The expected pdf of the mean was then obtained for each bin as the distribution of the mean values of the stopping power from the different experiments. For each pdf two 68 % probability intervals for the expected result were derived: the central interval, obtained by discarding 16 % of the results on each tail of the pdf, and the interval of minimum width containing 68 % of the results; this last interval always contains the most probable value.

In the low-momentum bins of Fig. 4, where the distributions are nearly Gaussian, the two intervals tend to coincide, and they also correspond to the conventional estimate of the experimental error.

For bins above 100 GeV/c, the differences between the two intervals become increasingly significant. The increasing probability of large fluctuations in radiative energy losses, combined with the decreasing size of the event samples, cause the most probable values to be systematically lower than the expectation values. This trend is particularly marked in the highest momentum bin, where the expectation value lies outside the 68% probability interval.

The curve

$$(\mathrm{d}E/\mathrm{d}x)_{meas} = \alpha \left[\left(\frac{\mathrm{d}E}{\mathrm{d}x} \right)_{coll} + \beta \times \left(\frac{\mathrm{d}E}{\mathrm{d}x} \right)_{rad} \right],$$

where *coll* and *rad* label the predicted energy losses in $PbWO_4$ due to collisions with atomic electrons and radiative processes respectively [12], is fitted to experimental stopping power data using a binned maximum likelihood and the pdf described above. The parameters α and β account for the overall normalization of the energy scale and for the relative normalization of radiation and collision losses. With the adopted parameterization the β parameter, from which the critical energy is measured, is independent of the overall energy scale. The fit results in:

$$\alpha = 1.004^{+0.002}_{-0.003}\,(\text{stat.}) \pm 0.016\,(\text{syst.})$$
$$\beta = 1.07^{+0.05}_{-0.04}\,(\text{stat.}) \pm 0.6\,(\text{syst.}).$$

Adding statistical and systematic contributions in quadrature, it may be concluded from the above results that the energy scale is consistent with expectations within a systematic uncertainty of 1.6 %, with a 1.2 % contribution from the uncertainty on the energy scale dependence on the angle and on the clustering, and a 1.0 % contribution from uncertainty in containment corrections. This result is mainly determined by the precision of the measurements in the momentum region below 20 GeV/c, where radiation losses are marginal.

From the fit results, a muon critical energy of $160^{+5}_{-6}\,(\text{stat.}) \pm 8\,(\text{syst.})$ GeV is obtained, in agreement with the computed value of 169.5 GeV for $PbWO_4$ [12]. The systematic uncertainty includes a contribution of 4.5 GeV from the uncertainty of the containment corrections, dominated by the limited knowledge of the correction for radiation losses, and a contribution of 6 GeV due to the stability of the result against bias subtraction and event selection.

6. – Conclusions

The muon stopping power in $PbWO_4$ has been measured over the momentum range from 5 GeV/c to 1000 GeV/c. In the region corresponding to muon momenta less than 20 GeV/c, where collision losses dominate, the average energy deposited in the crystals is of order 300 MeV. Thus the agreement (to within 1-2 %) between the measured stopping power and the calculated values confirms that the energy calibration of the detector, previously determined with 120 GeV/c electrons, remains valid down to the sub-GeV scale.

From a comparison of the rate of collision losses with that of radiative losses, a first experimental determination of the muon critical energy has been obtained. The experimental value 160^{+5}_{-6} (stat.) $\pm$ 8.0 (syst.) GeV is in agreement with numerical calculations for this material.

REFERENCES

[1] CMS Collaboration, *The CMS experiment at the CERN LHC*, *JINST*, **0803** (2008) S08004, doi:10.1088/1748-0221/3/08/S08004
[2] CMS Collaboration, *The CMS CRAFT Exercise*, *submitted to JINST*, (2009)
[3] CMS Collaboration, *Performance and Operation of the CMS Crystal Electromagnetic Calorimeter*, *submitted to JINST*, (2009)
[4] CMS Collaboration, *Studies of CMS Muon Reconstruction Performance with Cosmic Rays*, *submitted to JINST*, (2009)
[5] CMS Collaboration, *Commissioning of the CMS High-Level Trigger with Cosmic Rays*, *submitted to JINST*, (2009)
[6] Adzic P. et al., *Intercalibration of the barrel electromagnetic calorimeter of the CMS experiment at start-up*, *JINST*, **3** (2008) P10007, doi:10.1088/1748-0221/3/10/P10007
[7] GEANT4 Collaboration, Agostinelli S. et al., *GEANT4: A simulation toolkit*, *Nucl. Instrum. Meth.*, **A506** (2003) 250-303, doi:10.1016/S0168-9002(03)01368-8
[8] Almeida N. et al., *Data filtering in the readout of the CMS electromagnetic calorimeter*, *JINST*, **3** (2008) P02011, doi:10.1088/1748-0221/3/02/P02011
[9] Groom Donald E., Mokhov Nikolai V. and Striganov Sergei I., *Muon stopping power and range tables 10-MeV to 100-TeV*, *Atom. Data Nucl. Data Tabl.*, **78** (2001) 183-356, doi:10.1006/adnd.2001.0861
[10] Ivanov D., Kuraev E. A., Schiller A. and Serbo V. G., *Production of e+ e- pairs to all orders in Z alpha for collisions of high-energy muons with heavy nuclei*, *Phys. Lett. B*, **442** (1998) 453-458, arXiv:hep-ph/9807311, doi:10.1016/S0370-2693(98)01278-7
[11] Particle Data Group, Amsler C. et al., *Review of particle physics*, *Phys. Lett. B*, **667** (2008) 1, doi:10.1016/j.physletb.2008.07.018
[12] Particle Data Group, *Atomic and Nuclear Properties of Materials*, *web pages at: http://pdg.lbl.gov/2009/AtomicNuclearProperties/*, (2009)